

Figure 4. DSC study of the Mg_2CoH_3 phase transformation from the tetragonal to the cubic variety.

trace amounts of air present. Figure 3a shows the conductivity variation of the high-pressure hydride as a function of hydrogen pressure. Such a pressure dependence usually characterizes the hydriding of metals or metallic alloys.

The conductivity of the low-pressure hydride was measured on pellets that did not contain either the high-pressure hydride or any significant amount of impurity, as verified by X-ray diffraction. The measurements were carried out in a temperature range varying from 285 to 500 K (curve AB in Figure 3b). Prior to the measurements the samples were treated under 2-MPa hydrogen pressure at room temperature so as to stabilize the initial conductivity value (point A). The conductivity increases with rising temperature. The same shape for the conductivity curve is obtained in the temperature range considered, whatever the pressure.

But at 2-MPa hydrogen pressure and at a temperature of 500 K for 2 days, the low-pressure hydride is transformed into the high-pressure one. This phenomenon corresponds to a slight increase of the conductivity (from the B to the D point). Now the temperature change in the 570–300 K domain leads to the conductivity curve CDEF. The phase transformation from a tetragonal to a cubic symmetry reported earlier³ resulted in a conductivity jump around 470 K.

The phase transformation was found to be reversible from the conductivity measurements as well as by DSC measurements (Figure 4) with $\Delta H \approx 0.5 \text{ kcal mol}^{-1}$.

The conductivity was measured for samples of the tetragonal high-pressure phase synthesized at 4 MPa and 670 K. The conductivity curve obtained exhibits a similar shape.

The conductivity measurements imply a non-metallic character for both high- and low-pressure hydrides. As mentioned above, the low-pressure hydride can be transformed into the high-pressure one at rising temperature in agreement with the phase diagram (Figure 2) at 630 K and under 3–4-MPa hydrogen pressure. The reverse reaction also can take place, but the presence of MgH_2 is necessary.

Thermal decomposition of both hydrides has been carried out under vacuum for 4 days at various temperatures between 698 and 723 K. It always results in the formation of the intermetallic compound Mg_xCo in addition to magnesium and cobalt. It is very difficult to separate the phases present in the mixture after decomposition, so that the exact composition of the alloy could not be determined with sufficient accuracy. However, an electron microprobe analysis gave an atomic ratio corresponding approximately to a Mg_2Co composition. The existence of Mg_2Co has been previously reported⁶ but was not confirmed,⁷ so that its structure is still unknown. Mg_xCo cannot be obtained either by melting or by mechanical alloying in contrast to Mg_2Ni , which has been recently obtained by both methods.^{4,8}

Table II. X-ray Data for Mg_xCo

<i>hkl</i>	d_{obs} , Å	d_{calc} , Å	I_{obs}
111	6.61	6.599	100
220	4.04	4.04	6
400	2.856	2.587	1
422	2.333	2.333	12
511–333	2.198	2.199	70
440	2.020	2.020	23
531	1.932	1.932	5
600–442	1.904	1.905	15
620	1.806	1.807	5
533	1.741	1.743	8
622	1.721	1.723	8
733	1.395	1.396	2
660–822	1.345	1.347	9
751–555	1.319	1.319	4
842	1.248	1.247	3
931	1.1983	1.1982	2

The question is still open whether this intermetallic compound is a metastable phase that is stabilized by the presence of a certain amount of hydrogen or an intermetallic compound thermodynamically stable under our conditions.

Table II presents the X-ray data for Mg_xCo , which has been indexed with a face-centered cubic cell ($a = 11.43 \pm 0.01 \text{ Å}$).

There is a great difference between the behavior of Mg_xCo and that of a 2 Mg–Fe mixture during hydriding–dehydriding cycling. While the hydrogen storage capacity of the 2 Mg–Fe mixture decreases quickly, that of Mg_xCo remains almost the same after 50 cycles. This could result from the fact that Mg_xCo does not disproportionate while dehydriding of Mg_2FeH_6 leads to a mixture of elemental magnesium and iron. The consequence is a looser contact between Mg and Fe pairs along the absorption–desorption cycles. This phenomenon would account for the observed decrease of the hydrogen storage capacity.

Conclusion

By direct interaction of Mg and Co under hydrogen pressure we could synthesize two different ternary hydrides. We have studied the P – T diagram of the Mg–Co– H_2 system. The powder diffraction pattern corresponding to the high-pressure hydride is similar to that of the tetragonal phase reported earlier by Zolliker et al.³ In addition the existence of a low-pressure hydride has been established. It has been indexed with a hexagonal cell. Thermal decomposition of both hydrides leads to the formation of the new intermetallic compound Mg_xCo . A more detailed study is indeed required to determine the exact composition of this compound and to show how much it contains some residual hydrogen able to stabilize it.

Registry No. Mg, 7439-95-4; Co, 7440-48-4; H_2 , 1333-74-0; Mg_2Co , 12139-68-3; Mg_2CoH_3 , 98586-77-7.

Contribution from the Department of Chemistry, D-006,
University of California at San Diego,
La Jolla, California 92093

Synthesis, Structure, and Physical Properties of Tetrakis(μ -diphenyl phosphato)dimolybdenum(II)

Janet R. Morrow and William C. Troglor*

Received July 22, 1988

Scant structural information is available about the coordination of phosphate diesters to two metal centers. Recently the structure of $\{\text{Fe}_2\text{O}[\text{O}_2\text{P}(\text{O}Ph)_2]_2(\text{HB}(\text{pz})_3)_2\}$ was described;¹ it contains two diphenyl phosphate ligands bridging the Fe–O–Fe unit. This structure may provide a model for substrate binding pertinent to

(6) Cramer, E. M.; Nielsen, H. P.; Schonfeld, F. W. *Light Met. Age* 1947, 5(2), 1947, 6.

(7) Samsonov, G. V.; Perminov, V. P. *Magnides*; Mankowa Dumka: Kiev, USSR, 1971.

(8) Stepanov, A.; Ivanov, E. J.; Konstanchuk, J.; Boldyrev, V. J. *Less-Common Met.* 1987, 131, 89.

(1) Armstrong, W. H.; Lippard, S. J. *J. Am. Chem. Soc.* 1985, 107, 3730.

the phosphatase activity of uteroferrin² and the purple acid phosphatases,³ which also appear to contain the (μ -oxo)diiron(III) center. There has also been interest in the development of metal ion catalysts for the hydrolysis of phosphate diesters⁴ and DNA.⁵ From organophosphate ester chemistry it is well-known⁶ that incorporation of a five-membered ring (e.g. in PO_2^- ($\text{OCH}_2\text{CH}_2\text{O}^-$)) in the structure about phosphorus greatly accelerates phosphate ester hydrolysis. Therefore, we questioned whether a phosphate diester ligand could bridge two directly connected metal centers and whether this would activate the phosphodiester toward nucleophilic attack. Herein we describe a complex that contains diphenyl phosphate bridging a Mo–Mo quadruple bond.

Experimental Section

Molybdenum hexacarbonyl, acetic acid, sodium acetate, and diphenyl phosphate were purchased from commercial sources and used without purification. Tetrahydrofuran was distilled from potassium, methanol was distilled from magnesium, and diethyl ether and hexanes were distilled from sodium benzophenone ketyl. Trifluoromethanesulfonic acid was distilled under reduced pressure and stored under N_2 . Lithium dimethyl phosphate was synthesized by overnight reflux of trimethyl phosphate with lithium chloride in acetone. The free acid was obtained by acidification of an aqueous solution of lithium dimethyl phosphate to pH \sim 0 with concentrated HCl, followed by extraction with chloroform. The chloroform layer was dried over Na_2SO_4 and evaporated to dryness, and the liquid dimethyl phosphoric acid was desiccated over P_2O_5 for several days. $\text{Mo}_2(\text{OAc})_4$ ⁷ and $\text{Mo}_2(\text{OTf})_4$ ⁸ (OAc = acetate, OTf = trifluoromethanesulfonate) were synthesized as described in the literature. Crude $\text{Mo}_2(\text{OTf})_4$ was isolated as a beige powder after removal of excess trifluoromethanesulfonic acid in vacuo and used without further purification. All manipulations with molybdenum dimers were performed under an atmosphere of nitrogen by using standard Schlenk techniques.

Instrumentation. All ^{31}P and ^1H NMR spectra were recorded with use of a General Electric-QE 300-MHz spectrometer. Probe temperature was approximately 28 °C. Chemical shifts are referenced to external 85% phosphoric acid. Visible spectra were recorded with use of an IBM 9420 UV-vis spectrophotometer, and near-IR spectra were recorded on a Cary 14 spectrophotometer. EPR measurements were performed on a Varian E-3 X-band 9.141-GHz spectrometer at 77 K. Magnetic field strength was calibrated by use of diphenylpicrylhydrazyl as standard ($g = 2.0037$). For computer simulations of EPR spectra the program SIM14⁹ was run on an IBM 9000 computer. Electrochemical experiments were performed under nitrogen with the use of a BAS100 electrochemical analyzer by previously described procedures.¹⁰

Synthesis of Tetrakis(diphenyl phosphato)dimolybdenum(II), ($\text{Mo}_2(\text{DPP})_4(\text{THF})_2$). To 1 g of $\text{Mo}_2(\text{OTf})_4$ was added an 8-fold excess of $(\text{C}_6\text{H}_5\text{O})_2\text{PO}_2\text{H} = \text{DPPH}$ in 15 mL of dry methanol. The resulting pink solution was stirred for 5 min and evaporated to dryness in vacuo. The pink solid was washed with 50 mL of diethyl ether and recrystallized from THF and diethyl ether. Salmon pink highly air-sensitive crystals were obtained in 85% yield based on the amount of $\text{Mo}_2(\text{OAc})_4$ used to prepare $\text{Mo}_2(\text{OTf})_4$. ^{31}P NMR (THF- d_6): δ 5.03. ^1H NMR (THF- d_6): δ 1.75 (m), 3.30 (m), 7.73 (m). UV-vis (THF): $\lambda = 520$ nm ($\epsilon = 160$ $\text{M}^{-1}\text{cm}^{-1}$), 410 nm ($\epsilon = 76$ $\text{M}^{-1}\text{cm}^{-1}$). Anal. Calcd for $\text{C}_{56}\text{H}_{56}\text{O}_{18}\text{P}_4\text{Mo}_2$: C, 50.47; H, 4.24; P, 9.30; Mo, 14.4. Found: C, 49.23; H, 4.06; P, 9.24; Mo, 14.2.

Synthesis of $[\text{Mo}_2(\text{DPP})_4]\text{PF}_6$. To 0.40 g (0.30 mM) of $\text{Mo}_2(\text{DPP})_4$ dissolved in 10 mL of THF was added a THF solution of $[\text{Cp}_2\text{Fe}]\text{PF}_6$

Table I. Crystallographic Data for $\text{Mo}_2(\text{DPP})_4(\text{THF})_2$

chemical formula: $\text{C}_{56}\text{H}_{56}\text{O}_{18}\text{P}_4\text{Mo}_2$	fw = 1332.835
space group: $P\bar{1}$	$T = 23$ °C
$a = 10.682$ (3) Å	$\lambda = 0.71073$ Å
$b = 12.327$ (3) Å	$\rho_{\text{calc}} = 1.52$ g/cm ³
$c = 13.458$ (4) Å	$\mu = 5.94$ cm ⁻¹
$\alpha = 63.92$ (2) Å	$R(F_o^2) = 0.0575$
$\beta = 67.85$ (2) Å	$R_w(F_o^2) = 0.0696$
$\gamma = 87.23$ (2) Å	
$V = 1459.6$ Å ³	
$Z = 1$	

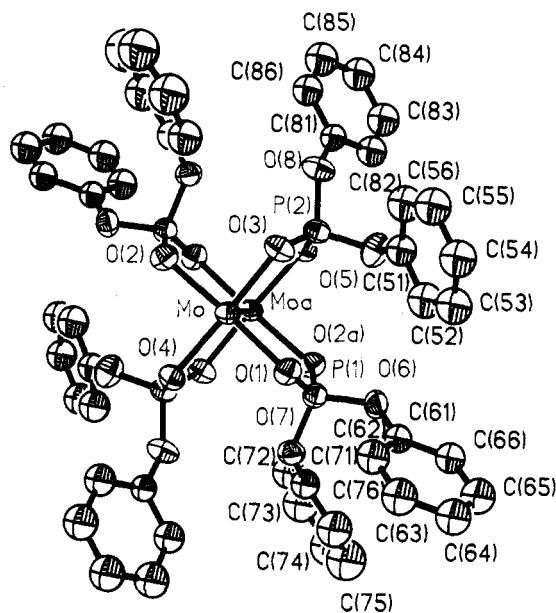


Figure 1. Thermal ellipsoid plot (50% ellipsoids) for the $\text{Mo}_2[\text{O}_2\text{P}(\text{O}-\text{C}_6\text{H}_5)_2]_4$ unit showing the atom-labeling scheme. Symmetry equivalent atoms (denoted by an a) are generated by the crystallographic inversion center located midway between Mo and Mo(a).

(0.10 g, 0.30 mM).¹¹ The yellow solution was stirred for several minutes and solvent was removed in vacuo. A silver-white air-sensitive powder was obtained after washing with hexane to remove Cp_2Fe (65% yield) UV-vis (THF): $\lambda = 640$ nm ($\epsilon = 44$ $\text{M}^{-1}\text{cm}^{-1}$), 440 nm ($\epsilon = 180$ $\text{M}^{-1}\text{cm}^{-1}$), 300 nm ($\epsilon = 890$ $\text{M}^{-1}\text{cm}^{-1}$). Near-IR (THF): 1530 nm ($\epsilon = 140$ $\text{M}^{-1}\text{cm}^{-1}$). Anal. Calcd for $\text{C}_{48}\text{H}_{40}\text{O}_{16}\text{P}_5\text{F}_6\text{Mo}_2$: C, 43.23; H, 3.02. Found: C, 42.71; H, 2.86.

Attempted Base Hydrolysis of $\text{Mo}_2(\text{DPP})_4$. The following reactions were performed in THF- d_8 and monitored by using ^{31}P NMR spectroscopy. Addition of 1 M NaOH immediately gave free DPP^- and a brown precipitate. Treatment with 10^{-2} M NaOH/10% $^{18}\text{O}_2$ immediately resulted in the formation of a brown precipitate. The aqueous solution (1 mL) was purified by passing the solution through a small alumina column (0.5 cm \times 2 cm). No incorporation of ^{18}O into free DPP^- was detected by using ^{31}P NMR spectroscopy ($<3\%$ ^{18}O incorporation into DPP^-).

Structure Determination of $\text{Mo}_2(\text{DPP})_4(\text{THF})_2$. A $0.1 \times 0.3 \times 0.1$ mm crystal of $\text{C}_{56}\text{H}_{56}\text{O}_{18}\text{P}_4\text{Mo}_2$ was mounted in a thin-walled quartz capillary, and 50 random reflections were found and centered (Nicolet R3m/V diffractometer); these reduced to a triclinic unit cell (Table I). Details of the data collection and refinement are given in Supplementary Table I. Data were corrected for a gradual decay observed for the standards to 83% of their original intensity. The SHELXTL PLUS program package (Nicolet Instruments Inc., Madison, WI) was used for data reduction and structure solution. The structure was solved by direct methods, and successful convergence (largest shift/esd for 170 least-squares variables = 0.001) was obtained in the centrosymmetric space group $P\bar{1}$ for 2822 unique reflections ($F > 6.0\sigma(F)$). All nonhydrogen atoms were refined anisotropically except for the phenyl rings, which were treated as isotropic rigid groups with fixed hydrogens (0.09 Å² fixed isotropic thermal parameter). One disordered phenyl ring (C(51)–C(56)) successfully refined between two sites of 0.71 and 0.29 occupancy. Be-

- (2) Pyrz, J. W.; Sage, J. T.; Debrunner, P. G.; Que, L., Jr. *J. Biol. Chem.* **1986**, *261*, 11015.
- (3) Antanaitis, B. C.; Aisen, P. *Adv. Inorg. Biochem.* **1983**, *5*, 111. Lippard, S. J. *Angew. Chem., Int. Ed. Engl.* **1988**, *27*, 344.
- (4) (a) Menger, F. M.; Gan, L. H.; Johnson, E.; Durst, D. H. *J. Am. Chem. Soc.* **1987**, *109*, 2800. (b) Chin, J. K.; Xiang, Z. *J. Am. Chem. Soc.* **1988**, *110*, 223. (c) Morrow, J. R.; Trogler, W. C. *Inorg. Chem.* **1988**, *27*, 3387.
- (5) Basile, L. A.; Raphael, A. L.; Barton, J. K. *J. Am. Chem. Soc.* **1987**, *109*, 7550.
- (6) Westheimer, F. H. *Chem. Rev.* **1981**, *81*, 313. Westheimer, F. H. *Science* **1987**, *235*, 1173.
- (7) Brignole, A. B.; Cotton, F. A. *Inorg. Synth.* **1972**, *13*, 81.
- (8) Abbott, E. H.; Schoenewolf, F. Jr.; Backstrom, T. J. *Coord. Chem.* **1974**, *3*, 255.
- (9) Lozos, G. P.; Hoffmann, B. M.; Franz, C. G. *QCPE* **1974**, *No. 11*, 265.
- (10) Holland, G. F.; Ellis, D. E.; Trogler, W. C. *J. Am. Chem. Soc.* **1986**, *108*, 1884. Therien, M. J.; Trogler, W. C. *J. Am. Chem. Soc.* **1987**, *109*, 5127.

- (11) Following the procedure of Hendrickson et al. (Hendrickson, D. N.; Sohn, Y. S.; Gray, H. B. *Inorg. Chem.* **1971**, *10*, 1559), with recrystallization from acetone/hexane.

Table II. Atomic Coordinates ($\times 10^4$) and Equivalent Isotropic Displacement Parameters ($\text{\AA}^2 \times 10^3$) for $\text{Mo}_2(\text{DPP})_4(\text{THF})_2$

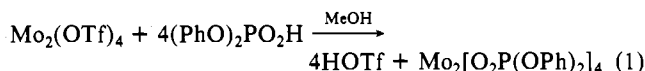
	x	y	z	$U(\text{eq})^a$
Mo	-88 (1)	130 (1)	758 (1)	34 (1)
P(1)	-2326 (3)	1270 (2)	-157 (2)	41 (1)
P(2)	-1750 (3)	-2333 (2)	1601 (2)	41 (1)
O(1)	-1933 (6)	938 (5)	888 (5)	43 (3)
O(2)	1716 (6)	-625 (5)	915 (5)	45 (3)
O(3)	-1267 (6)	-1625 (5)	2085 (4)	43 (3)
O(4)	1062 (6)	1921 (5)	-270 (5)	41 (3)
O(5)	-3315 (7)	-2326 (6)	1891 (5)	60 (4)
O(6)	-3923 (6)	1007 (5)	258 (6)	51 (4)
O(7)	-1949 (7)	2701 (5)	-910 (5)	47 (3)
O(8)	-1568 (7)	-3692 (5)	2329 (5)	52 (3)
C(52)	-5145 (11)	-1527 (8)	2885 (7)	75
C(53)	-6123	-1549	3935	75
C(54)	-6251	-2473	5058	75
C(55)	-5400	-3375	5131	75
C(56)	-4422	-3353	4081	75
C(51)	-4295	-2429	2958	57 (4)
C(52')	-4315 (23)	-2627 (22)	3942 (23)	75
C(53')	-5459	-2622	4888	75
C(54')	-6612	-2175	4687	75
C(55')	-6620	-1733	3542	75
C(56')	-5476	-1738	2596	75
C(51')	-4324	-2185	2797	70
C(62)	-4628 (6)	2100 (6)	1475 (6)	66 (3)
C(63)	-5632	2677	1996	75 (3)
C(64)	-6874	2717	1872	72 (3)
C(65)	-7113	2180	1227	73 (3)
C(66)	-6109	1603	706	57 (3)
C(61)	-4866	1563	830	47 (2)
C(72)	-1269 (7)	3283 (7)	-3004 (7)	74 (3)
C(73)	-1427	3972	-4084	98 (4)
C(74)	-2446	4722	4117	104 (4)
C(75)	-3308	4784	-3071	115 (5)
C(76)	-3150	4095	-1991	86 (4)
C(71)	-2130	3345	-1958	56 (3)
C(82)	-2251 (7)	-4665 (6)	1339 (6)	64 (3)
C(83)	-2136	-5601	1006	77 (3)
C(84)	-1281	-6468	1310	77 (3)
C(85)	-541	-6398	1946	78 (3)
C(86)	-656	-5462	2278	62 (3)
C(81)	-1512	-4595	1975	45 (2)
O(9)	-621 (9)	294 (7)	2778 (7)	82 (2)
C(91)	-2010 (15)	147 (13)	3532 (12)	107 (5)
C(92)	-2214 (19)	-899 (16)	4719 (15)	154 (7)
C(93)	-928 (17)	-1345 (15)	4589 (14)	132 (6)
C(94)	108 (16)	-352 (13)	3486 (12)	114 (5)

^a Equivalent isotropic U defined as one-third of the trace of the orthogonalized U_{ij} tensor.

cause of the low absorption coefficient and crystal decay, an absorption correction was not applied. Final atomic positional and isotropic thermal parameters are given in Table II.

Results and Discussion

Addition of excess $(\text{PhO})_2\text{PO}_2\text{H}$ to $\text{Mo}_2(\text{OAc})_4$ only led to partial replacement of the acetate ligands; however, by using the triflate ($\text{O}_3\text{SCF}_3^- = \text{OTf}$) complex complete substitution occurred (eq 1). The diphenyl phosphate ligand was labile to displacement



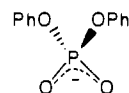
from the complex. Addition of aqueous NaOH (1 M), acetic acid (2 equiv), or $\text{HOP}(\text{O})(\text{OMe})_2$ (8 equiv) to a THF solution of the complex produced free DPP^- or DPPH as observed at $\delta -8.9$ to -10 in the ^{31}P NMR spectrum.

Crystals of $\text{Mo}_2(\text{DPP})_4 \cdot 2\text{THF}$ were obtained on recrystallization from THF, and the molecular structure is shown in Figure 1. The coordination geometry about the Mo_2^{4+} core adopts the eclipsed D_{4h} structure usually observed¹² in quadruply bonded complexes.

Table III. Selected Bond Lengths (\AA) and Angles (deg) in $\text{Mo}_2(\text{DPP})_4(\text{THF})_2$

Bond Lengths			
Mo-Mo(a)	2.141 (2)	P(1)-O(6)	1.583 (7)
Mo-O(1)	2.147 (6)	P(1)-O(7)	1.578 (6)
Mo-O(2)	2.142 (7)	P(2)-O(3)	1.500 (8)
Mo-O(3)	2.151 (5)	P(2)-O(4a)	1.500 (6)
Mo-O(4)	2.143 (5)	P(2)-O(5)	1.567 (8)
P(1)-O(1)	1.498 (8)	P(2)-O(8)	1.572 (6)
P(1)-O(2a)	1.503 (8)	Mo-O(9)	2.656 (9)
Bond Angles			
O(1)-Mo-O(3)	90.1 (2)	O(3)-P(2)-O(8)	105.3 (4)
O(1)-Mo-O(4)	89.3 (2)	O(3)-P(2)-O(4a)	116.7 (3)
O(2)-Mo-O(3)	89.0 (2)	O(3)-P(2)-O(5)	111.2 (4)
O(2)-Mo-O(4)	89.6 (2)	O(5)-P(2)-O(8)	106.4 (4)
O(1)-P(1)-O(7)	105.4 (4)	O(5)-P(2)-O(4a)	106.0 (4)
O(1)-P(1)-O(2a)	116.1 (4)	O(8)-P(2)-O(4a)	110.9 (4)
O(1)-P(1)-O(6)	112.0 (4)	Mo-O(1)-P(1)	115.1 (4)
O(6)-P(1)-O(7)	105.4 (4)	Mo-O(2)-P(1a)	114.4 (6)
O(6)-P(1)-O(2a)	105.2 (4)	Mo-O(3)-P(2)	115.3 (3)
O(7)-P(1)-O(2a)	112.5 (3)	Mo-O(4)-P(2a)	114.9 (4)

The short (2.141 (2) \AA) Mo-Mo bond also is typical of these complexes. Two THF molecules (not shown) are bound weakly in the axial positions of the complex with Mo-O(9) = 2.656 (9) \AA . Weak coordination of axial ligands is also a common occurrence¹² in the solid-state structures of dimolybdenum(II) complexes. Within the bridging $(\text{PhO})_2\text{PO}_2^-$ ligand, we observe (Table III) short P-O bond lengths 1.498 (8)-1.503 (8) \AA for the O(1)-O(4) oxygens bound to Mo and significantly longer P-O bonds 1.567 (8)-1.583 (7) \AA to the phenyl substituted oxygens. This agrees with the formulation of the phosphate ligand as a symmetrical bridging unit (similar to acetate):



The largest O-P-O angles belong to the atoms spanning the quadruple bond with O(1)-P(1)-O(2a) = 116.1 (4) $^\circ$ and O(3)-P(2)-O(4a) = 116.7 (3) $^\circ$. Most of the other O-P-O angles are closed up slightly from the tetrahedral value of 109 $^\circ$. In the structure of $[\text{Fe}_2\text{O}[\text{O}_2\text{P}(\text{OPh})_2]_2(\text{HB}(\text{pz})_3)_2]$, the diphenyl phosphate ligand symmetrically bridges the two Fe atoms linked by the μ -oxo bridge and the bridging O-P-O angle of 120.1 $^\circ$ is similarly expanded.¹ This contrasts with the structure reported for the bridging HPO_4^{2-} group in $[\text{Mo}_2(\text{HPO}_4)_4]^{2-}$ salts.¹³ Here the O-P-O angle bridging the two Mo atoms ranges from 106.2 (2) to 109.3 (5) $^\circ$, which is significantly less than in the phosphate diester complex.

The Mo_2O_2 portion of the five-membered $\text{Mo}_2\text{O}_2\text{P}$ ring is rigorously planar; however, P(1) and P(2) are displaced 0.257 and 0.197 \AA , respectively, from their corresponding Mo_2O_2 planes. Dihedral angles of 18.9 and 14.5 $^\circ$, respectively, characterize the ring puckering. Each metal chelate ring distorts in the same direction so approximate molecular C_{4h} symmetry is preserved. In this sense the structure resembles that of $\text{M}_2[(\text{CH}_2)_2\text{P}(\text{CH}_3)_2]_4$ for $\text{M} = \text{Cr}$ or Mo ,¹⁴ where the displacement of P from the $\text{M}_2\text{C}_2\text{P}$ ring led to dihedral angles of 17.1-19.9 $^\circ$.

The cyclic voltammogram of $\text{Mo}_2(\text{DPP})_4$ in THF solvent (0.1 M in tetra-*n*-butylammonium hexafluorophosphate) showed a single chemically reversible wave at a Pt electrode at +0.358 V vs a Ag-wire reference electrode or at -0.520 V vs internal ferrocene as a reference. Linear-sweep voltammetry established the wave to arise from oxidation of $\text{Mo}_2(\text{DPP})_4$. Both peak separations for the oxidation waves of Cp_2Fe and $\text{Mo}_2(\text{DPP})_4$ were 120 mV at a 50 mV/s scan rate in the cyclic voltammetry experiment. Coulometry showed 1.1 electrons/dimer were transferred on oxidation. Chemical oxidation with 1 equiv of $[\text{Cp}_2\text{Fe}]\text{PF}_6$ pro-

(12) Cotton, F. A.; Walton, R. A. *Multiple Bonds Between Metal Atoms*; Wiley-Interscience: New York, 1982.

(13) Bino, A.; Cotton, F. A. *Inorg. Chem.* **1979**, *18*, 3562.

(14) Cotton, F. A.; Hanson, B. E.; Ilsley, W. H.; Rice, G. W. *Inorg. Chem.* **1979**, *18*, 2713.

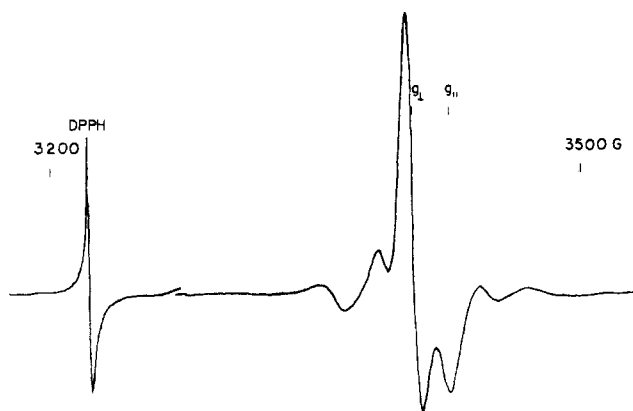


Figure 2. EPR spectrum of a 10^{-3} M frozen THF solution of $[\text{Mo}_2[\text{O}_2\text{P}(\text{OC}_6\text{H}_5)_2]_4][\text{PF}_6]$ at 77 K (9.141 GHz) with diphenylpicrylhydrazyl (DPPH) standard.

duced the mixed-valence species $[\text{Mo}_2(\text{DPP})_4]\text{PF}_6$ in 65% isolated yield. The cyclic and linear sweep voltammograms of this species showed a reduction wave at -0.52 V vs the ferrocene standard.

Physical properties of $\text{Mo}_2(\text{DPP})_4$ and $[\text{Mo}_2(\text{DPP})_4]\text{PF}_6$ resemble those of isoelectronic partners $\text{Mo}_2(\text{HPO}_4)_4^{4-}$ – $\text{Mo}_2(\text{HPO}_4)_4^{3-}$,^{13,15} and $\text{Mo}_2(\text{SO}_4)_4^{4-}$ – $\text{Mo}_2(\text{SO}_4)_4^{3-}$.^{16,17} The quadruply bonded complex exhibits a weak absorption assigned to the $\delta \rightarrow \delta^*$ transition at 520 nm ($\epsilon = 160 \text{ M}^{-1} \text{ cm}^{-1}$). On oxidation the $\delta \rightarrow \delta^*$ transition red-shifts in the mixed-valence complex to 1530 nm ($\epsilon = 140 \text{ M}^{-1} \text{ cm}^{-1}$), and vibronic structure corresponding to a 303-cm^{-1} progression (six members observed) in the Mo–Mo stretch is observed on the absorption in solution at room temperature. This is similar to $\text{Mo}_2(\text{SO}_4)_4^{3-}$, which absorbs at 1405 nm ($\epsilon = 143 \text{ M}^{-1} \text{ cm}^{-1}$) and exhibits a 350-cm^{-1} vibrational progression in solution, and to $\text{Mo}_2(\text{HPO}_4)_4^{3-}$, which absorbs at 1438 nm ($\epsilon = 180 \text{ M}^{-1} \text{ cm}^{-1}$) and exhibits a 334-cm^{-1} vibrational progression. The large charge difference between $\text{Mo}_2(\text{DPP})_4$ and $\text{Mo}_2(\text{SO}_4)_4^{4-}$ or $\text{Mo}_2(\text{HPO}_4)_4^{4-}$ allows the former complex to be dissolved in organic solvents, which may be useful in studies of the photoredox behavior¹⁵ of these complexes.

The magnetic properties of $\text{Mo}_2(\text{DPP})_4^{4+}$ also resemble those of the other mixed-valence Mo(II)–Mo(III) dimers.^{13,15–17} In THF solution the μ_{eff} of $[\text{Mo}_2(\text{DPP})_4]\text{PF}_6$ was $1.58 \mu_{\text{B}}$, determined by the Evans method. At 77 K in a THF glass an EPR spectrum (9.141 GHz) similar to that of $\text{Mo}_2(\text{SO}_4)_4^{3-}$ was observed (Figure 2) whose line shape could be fit by assuming $g_{\parallel} = 1.899$ and $g_{\perp} = 1.911$ and by assuming average hyperfine splitting constants from both ^{95}Mo and ^{97}Mo of $A_{\parallel} = 22.7 \text{ G}$ and $A_{\perp} = 12.8 \text{ G}$.

This work establishes the ability of $\text{PO}_2(\text{OPh})_2^-$ to bridge two metal centers in a dinuclear metal–metal-bonded complex. Qualitative observations suggest the ligand binds more weakly than acetate, but better than triflate. Nucleophilic attack by OH^- at phosphorus in the bound diester was not observed because of rapid cleavage of the ligand from the dinuclear center. In the context of using a dinuclear metal complex to introduce strain into a phosphate diester complex, this seems unlikely given the opening of the bridging O–P–O angle on binding. However, expanding the O–P–O angle toward 120° may stabilize a trigonal-bipyramidal transition state (with MO_2P equatorial), which is often invoked⁶ for nucleophilic substitutions at phosphorus. This strategy is being explored with less labile metal complexes.

Acknowledgment. This research was supported by the Army Research Office (Grant DAAG29-85-K0263). We thank the DoD University Research Instrumentation Program (Grant DAAL03-87-G-0071) for funds to purchase the X-ray diffractometer. We thank Prof. T. Don Tilley for helpful discussions and Prof. William H. Armstrong for providing additional crys-

tallographic data for the structure in ref 1.

Supplementary Material Available: Tables of crystallographic data, bond distances, bond angles, anisotropic displacement parameters, and hydrogen atom coordinates (7 pages); a table of observed and calculated structure factors (19 pages). Ordering information is given on any current masthead page.

Contribution from the Department of Chemistry, Purdue University, West Lafayette, Indiana 47907

Solid-State Structure of $[\text{Li}(\mu\text{-OAr-2,6-Ph}_2)_3\text{Sn}]$ (OAr-2,6-Ph₂ = 2,6-Diphenylphenoxide): A Cage Compound Containing a Pyramidal Lithium Atom

Glen D. Smith, Phillip E. Fanwick, and Ian P. Rothwell*¹

Received July 6, 1988

There has been a rapid growth of interest over the last few years in the solid-state structures adopted by main-group-element compounds.² Two areas of particular interest are the structural impact of sterically demanding functional groups³ and the importance of π -bonding between main-group elements and unsaturated organic systems.⁴ During our studies of the transition-metal chemistry associated with the sterically demanding aryloxy ligand 2,6-diphenylphenoxide (OAr-2,6-Ph₂), we have demonstrated an ability for this group to chelate to metal centers either through formation of a metal–carbon σ -bond or else via an η^6 -interaction involving one of the side-chain aryl groups.⁵ We have recently extended our studies of the chemistry of this and related ligands to derivatives of the main-group metals, and some complementary reactions involving CH bond activation have been uncovered.⁶ However, the purpose of this note is to describe the isolation and structure of the title compound, a five-membered-cage material that contains a formally three-coordinate lithium atom apparently stabilized by weak interactions with the side-chain aryl groups of three 2,6-diphenylphenoxide ligands.

Results and Discussions

The addition of 2 equiv of LiOAr-2,6-Ph_2 to SnCl_4 in benzene or toluene results in the formation of the cyclometalated dimer $[\text{Cl}_2\text{Sn}(\text{OC}_6\text{H}_3\text{Ph-C}_6\text{H}_4)]_2$ held together by bridging oxygen atoms.⁶ However, a second only slightly hydrocarbon-soluble minor product was also obtained as large colorless blocks from hot toluene. A solid-state X-ray diffraction analysis of this minor product (vide infra) showed it to have the stoichiometry $[\text{LiSn}(\text{OAr-2,6-Ph}_2)_3]$ (1) containing a Sn(II) metal center formed by reduction of Sn(IV) in the reaction mixture. Mass spectrometric data for this component showed a strong parent molecular ion, 1^+ , with no evidence for higher oligomers. A much more rational

- (15) Chang, I.-H.; Nocera, D. G. *J. Am. Chem. Soc.* **1987**, *109*, 4901, 4907.
 (16) Cotton, F. A.; Frenz, B. A.; Pedersen, E.; Webb, T. R. *Inorg. Chem.* **1975**, *14*, 391.
 (17) Erwin, D. K.; Geoffroy, G. L.; Gray, H. B.; Hammond, G. S.; Solomon, E. I.; Troglor, W. C.; Zagars, A. A. *J. Am. Chem. Soc.* **1977**, *99*, 3620.

- (1) Camille and Henry Dreyfus Teacher-Scholar, 1985–1990; Fellow of the Alfred P. Sloan Foundation, 1986–1990.
 (2) *Comprehensive Coordination Chemistry*; Wilkinson, G., Gillard, R. D., McCleverty, J. A., Eds.; Pergamon Press: Oxford, England, 1987; Vol. 3.
 (3) (a) Cowley, A. H. *Polyhedron* **1984**, *3*, 389. (b) Cowley, A. H. *Acc. Chem. Res.* **1984**, *17*, 384. (c) Hitchcock, P. B.; Lappert, M. F.; Miles, S. J.; Thorne, A. J. *J. Chem. Soc., Chem. Commun.* **1984**, 480. (d) Maxmore, S.; Sita, L. R. *J. Am. Chem. Soc.* **1985**, *107*, 6390. (e) Flynn, K. M.; Olmstead, M. M.; Power, P. P. *J. Am. Chem. Soc.* **1983**, *105*, 2085. (f) Veith, M. *Angew. Chem., Int. Ed. Engl.* **1987**, *26*, 1.
 (4) (a) Jutz, P. *Adv. Organomet. Chem.* **1986**, *26*, 217. (b) Jonas, K. *Adv. Organomet. Chem.* **1981**, *19*, 97.
 (5) (a) Kerschner, J. L.; Fanwick, P. E.; Rothwell, I. P. *J. Am. Chem. Soc.* **1987**, *109*, 5840. (b) Kerschner, J. L.; Rothwell, I. P.; Huffman, J. C.; Streib, W. *Organometallics*, in press.
 (6) Smith, G. D.; Rothwell, I. P. To be submitted for publication.